

Experiment 1: Drag Coefficient

Written Report

ME 370: Energy Systems Laboratory
TA: Eli Gaeta

Prepared By: Josephine Matyszewski, Eric Martin,
Matthew Wanty, Ethan Zoland

May 2, 2024

Table of Contents

Table of Contents	2
Nomenclature	3
Objectives	4
Executive Summary	4
Student's Roles	5
Introduction	5
Approach and Methods	6
Results and Discussion	8
Question 1: Inlet Pressure Drop	8
Question 2: Flow Separation	8
Question 3: Reynolds Number	10
Question 4: Rotational Directions	11
Question 5: Upstream Pitot vs Ambient	11
Question 6: Pressure Distributions	12
Question 7: Drag Force	14
Question 8: Drag Coefficient	14
Question 9: Sources of Error	16
Conclusions	17
Appendices	18
Appendix 1: Team Contract	18
Appendix 2: EES Code	19
Appendix 3: Hand Calculations	24
Appendix 4: Citations	25

Nomenclature

$A_{f,l}$	Frontal area of large cylinder
$A_{f,s}$	Frontal area of small cylinder
C_D	Drag coefficient
$C_{D,mom}$	Drag coefficient, momentum method
$C_{f,bar}$	Average shear stress coefficient
d_{large}	Diameter of large cylinder
d_{small}	Diameter of small cylinder
$F_{D,l}$	Drag force on large cylinder
$F_{D,mom}$	Drag force, momentum method
$F_{D,s}$	Drag force on small cylinder
L	Length of cylinder
P	Pressure
P_{amb}	Ambient pressure
P_{diff}	Pressure differential
P_{dyn}	Dynamic pressure
P_{large}	Pressure on surface of large cylinder
P_{small}	Pressure on surface of small cylinder
P_{stag}	Stagnation pressure
Re_D	Reynolds number
r	Radius
T_{amb}	Ambient temperature
vel_{down}	Downstream velocity
vel_{up}	Upstream velocity
$v_{inf,avg}$	Average free stream velocity
μ	Viscosity
ρ_1	Density
ρ_2	Density
τ_{wall}	Shear force on wall



Objectives

The primary objective of this experiment is to examine the drag coefficient of cylinders in different airflow situations within a wind tunnel, paying particular attention to how various surface textures and sizes impact this measurement. The research seeks to enhance comprehension of how changes in Reynolds numbers affect the airflow behavior around the cylinder, especially during the shift from laminar to turbulent flow.

Executive Summary

This experiment explores the fundamental principles governing drag forces acting on bodies immersed in fluid flow. By focusing on the pressure and velocity characteristics of a cylinder placed perpendicularly to airflow in a wind tunnel, the relationships between cylinder size, surface roughness, drag coefficient and force can be realized. This report presents two methods of determining these relationships: the pressure distribution method and the momentum flux method.

In addition to performing both methods for determining drag forces and coefficients, the flow's boundary layers, separation points, and laminar-to-turbulent characteristics were analyzed. Knowledge on pitot tubes was also reinforced with fundamental static, dynamic, and stagnation pressure measurements. This report allows for a better understanding of fluid flow, building on both a theoretical and practical basis, with the drag force and coefficient results tabulated below.

Cylinder Size	Drag Coefficient [-]	Drag Force [N]
Small	1.22	3.9
Large	0.76	8.0

Understanding these principles and the effects drag forces can have on design optimization is crucial for various engineering applications, from wind turbine technology to aerospace applications. By applying and learning about these principles in an experimental setting, such as wind tunnel tests, professionals can accurately predict and minimize drag forces and increase performance.

Student's Roles

For experiment 1, each member of the team contributed different aspects to the data collection and report. Matt and Eric completed the EES and data analysis for the experiment. Josie and Ethan handled the formatting and writing of the report. Ethan wrote the nomenclature, objectives, student roles, introduction, and approach and methods section. Josie wrote the executive summary and conclusions. The results and discussion section was split evenly between all group members.

Introduction

Cylinders are fundamental shapes in various engineering fields, utilized in everything from fluid dynamics studies to architectural designs. Their relevance is particularly pronounced in aerodynamics, where understanding airflow dynamics around cylindrical objects can significantly influence the design and efficiency of vehicles, including cars and aircraft. This experiment is focused on examining the drag coefficient of cylinders under various airflow conditions in a wind tunnel, aiming to explore how different surface textures and sizes affect this parameter.

Cylinders offer a straightforward yet effective medium to study the transition from laminar to turbulent flow, a critical aspect of fluid dynamics. The study of this transition is essential for predicting the behavior of air around objects and can be applied to enhance performance in automotive aerodynamics and aircraft design. Specifically, this experiment investigates how changes in Reynolds numbers influence airflow dynamics, focusing on the crucial shift from laminar to smooth turbulent flow around the cylinder.

To achieve the outlined objectives, the experiment employs two primary testing methods: the Pressure Distribution Method and the Momentum Flux Method. These methods are chosen for their effectiveness in measuring the critical parameters involved in airflow dynamics. The Pressure Distribution Method involves analyzing pressure variations around the cylinder, while the Momentum Flux Method calculates the momentum flux across a control volume around the object, providing comprehensive data on how airflow interacts with the cylinder's surface.

The equipment used for this experiment is centered around a sophisticated open-circuit, subsonic wind tunnel. This facility is equipped to handle cylinders of various sizes and features adjustable settings to manipulate airflow velocity and turbulence levels. Data collection is facilitated by a Labview-based instrumentation system, which utilizes Pitot tubes to record pressure and flow dynamics, ensuring accurate and reliable measurements.

Overall, this experiment not only aims to enrich academic understanding in fluid mechanics but also seeks to offer practical insights that can be directly applied to optimize

designs in the automotive and aerospace industries. The careful selection of test methods and equipment underscores the experiment's commitment to delivering precise and actionable results, contributing to both theoretical knowledge and practical applications in engineering.

Approach and Methods

To determine the drag coefficient of the cylinders, measurements need to be made. The experimental setup is illustrated in Figure A-1. Air is drawn through entrance screens by a fan and moves over the test section containing the test cylinder. As the air flows around the cylinder, measurements are recorded through an inlet tube on the cylinder. The air then flows through a diffuser and back to the fan.

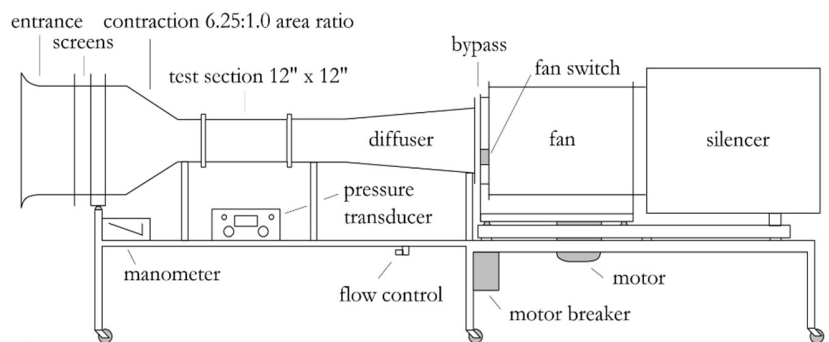


Figure 1. Locations of Pressure Measurements

The pitot tube setup is depicted in Figure A-2, where air flows around the cylinder within the test section and is captured using a pitot tube to measure the stagnation and static pressures of the free stream.

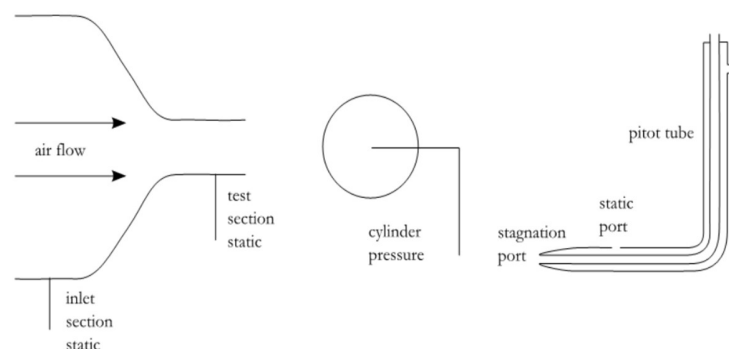


Figure 2. Pitot Tube Setup

The process of obtaining these measurements started with the setup and validation of the experiment. A thorough inspection of the wind tunnel and its components was carried out to confirm they were operating properly and securely. This involved ensuring that the fan and other mechanical elements were defect-free and properly aligned. Prior to conducting any tests, it was necessary to calculate the pressure drop needed to achieve speeds of 30 and 35 meters per second (m/s). This calculation was performed using Bernoulli's equation, equation 1.26, together with the continuity equation, equation 1.29 (both from the lab manual).

$$P_0 + \frac{1}{2}\rho_0 v_0^2 = P_s + \frac{1}{2}\rho_s v_s^2. \quad (1.26)$$

$$A_1 v_1 = A_2 v_2 \quad (1.29)$$

With this, two equations and two unknowns are able to be solved simultaneously to reveal the required pressure drop. Once the pressure drop was dialed, the runs could commence.

The initial test, aimed at capturing the free stream profile, began with the installation of the smooth cylinder, ensuring the sides were not scratched during the process. The ambient temperature and pressure were documented, the Labview file was set up, and the wind tunnel fan was activated. The crank under the diffuser section was adjusted to achieve a pressure drop of about 530 Pascals (Pa), corresponding to a velocity of 30 m/s. The "Upstream Pitot" Labview file was activated, and the pitot tube was moved across the vertical length of the test section. Additionally, measurements were taken using the momentum flux method, which involved readings from both upstream and downstream pitot probes. The downstream measurements were carried out by selecting the "Downstream Pitot" Labview file and maneuvering the downstream pitot tube in a manner similar to the upstream procedure. This was then repeated with a pressure drop of 720 Pa, corresponding to a velocity of 35 m/s.

To measure using the pressure distribution method, the fan's speed was maintained. Data collection began via the "Small Cylinder" tab in Labview, starting with the cylinder's hole at the bottom and rotating the small cylinder clockwise for one and a half turns. Subsequently, with the hole now on top, the small cylinder was rotated counterclockwise for the same number of turns. After this, the small cylinder was carefully switched out for the large cylinder, and similar rotational procedures were followed using the "Large Cylinder" tab in Labview. After obtaining all data from the above tests, calculations were completed in order to determine the drag coefficients and flow characteristics over the small and large cylinders.

Results and Discussion

1. Is the pressure drop across the inlet contraction the same as the measured dynamic pressure at the test section inlet?

The pressure drop across the inlet contraction is within 1% of the value for the measured dynamic pressure. These were both calculated and taken from the upstream pitot probe at the center of the tunnel (y-location of 0 meters), and are summarized in table 1-1.

Table 1-1. Calculated and measured values of inlet pressure.

<i>Calculated $P_{\text{drop,inlet}}$</i> [Pa]	<i>Measured P_{dynamic}</i> [Pa]
530.7	537

In theory, these numbers should be the same. This is because dynamic pressure represents the fluid's velocity, a parameter that is increased by the inlet contraction. Calculating the inlet pressure drop was vital in determining the operating pressure gradient for the experiment, so the details of the calculation can be found in the beginning of the Approach and Methods section.

2. Explain how C_p values from the pressure distribution data reflect the boundary layer velocity. What feature in your data indicates flow separation?

The pressure coefficient, C_p , is a direct indicator of boundary layer velocity. To prove this relationship, it helps to visualize airflow over the cylinder in figure 2-1.

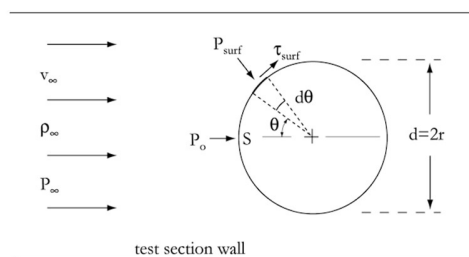


Figure 2-1. Fluid flow parameters over fixed cylinder (side view).

Here, point S represents the stagnation point, at which the fluid flow is brought to rest. If fluid is at rest, there is no pressure differential to drive the fluid flow, and C_P here is equal to 1. In other words, the pressure at the cylinder surface is equal to the dynamic pressure in the fluid, giving a ratio equal to 1. Air moving around the cylinder, farther from point S and towards the top, increases in velocity. According to Bernoulli's equation, this will lead to a decrease in pressure and thus a decreasing C_P . This is seen in both the ideal case and the observed data, shown in figure 2-2.

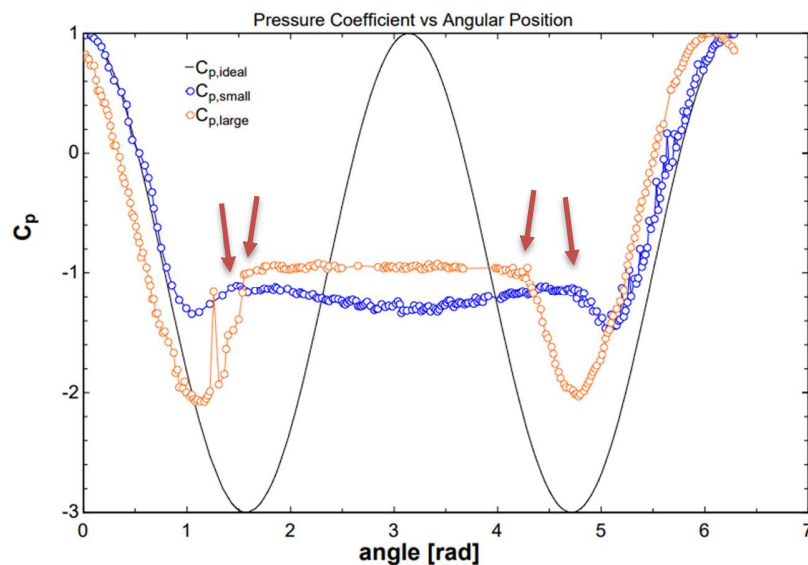


Figure 2-2. Observed pressure coefficients for inviscid, small, and large cylinders (error bars indicate uncertainty, red arrows indicate flow separation).

This trend in the experimental data (blue and orange) only holds until 1-2 radians. To explain this, we can look at the ideal case (black). Under inviscid conditions, as the flow reaches the top of the cylinder ($\pi/2$ radians or 90 degrees), the minimum surface pressure and minimum C_P is reached. The reason the observed data does not reach as low of a minimum as the ideal case is because air is not inviscid. Viscous dissipation causes the airflow to lose momentum as it traverses the cylinder. Once enough momentum is lost, the air no longer has enough energy to maintain the path of the cylinder, and it must separate. The blue and orange lines show this separation point at around 1.5 radians (indicated by the red arrows), a bit before the top of the cylinder.

The flat region indicates the separated region on the “back” of the cylinder, at which C_P is held constant. This is due to the flow being completely separated off the back, leading to a lack of changing pressure. As the cylinder rotation comes back around, the flow separation on the “bottom” side of the cylinder can be observed at around 4.5-5 radians.

3. Is the flow near the cylinder surface laminar or turbulent before the points of separation? Is the separation point where you would expect it to be based on the Reynolds number?

With the critical Reynolds number (Re) for external flow being 5×10^5 , the calculated Re values for flow over both small and large cylinders with 30 m/s stream velocity can be compared in table 3-1.

Table 3-1. Calculated Reynolds numbers for flow over small and large cylinders.

$Re_{d,small}$ [-]	$Re_{d,large}$ [-]
3.9×10^4	1.04×10^5

The Reynolds numbers indicate that the small cylinder encounters laminar flow while the large cylinder encounters a laminar-to-turbulent transition - occurring between Re values from $10^5 - 5 \times 10^5$. During this transition, the separation point jumps from less than 90 degrees to greater than 90 degrees, which is observed in figure 2-2. Laminar separation points occur below 90 degrees, also observed in figure 2-2. Figure 3-1 shows the pressure coefficients versus position for inviscid and actual flow, and a direct comparison to figure 2-2 proves the results to be sound.

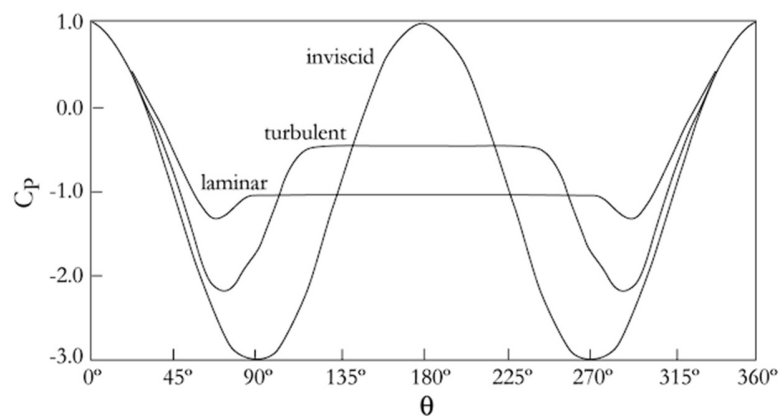


Figure 3-1. Pressure coefficient of actual and inviscid flows versus position.

These results also make intuitive sense, as the large cylinder has significant roughness that triggers turbulence. Additionally, the flow separation occurs farther up the cylinder because the mixing of fluid that turbulence induces actually gives the flow slightly more momentum.

4. Comment on the difference between the pressure distribution data gathered in the clockwise and counterclockwise directions.

The primary reasons that no difference would be observed between clockwise and counterclockwise rotation are that the cylinder is symmetrical and the rotations during the experiment were done very slowly. With slow rotations, no angular momentum could be transferred to the fluid, which would potentially alter the pressure profiles. Additionally, because of the cylinder's symmetry, there is no opportunity for a pressure differential to be generated between the top and bottom, and thus no lift can be generated, something that would be indicated by a difference in direction of rotation.

5. Are the static and stagnation pressures measured by the upstream Pitot probe at the center of the wind tunnel lower, greater, or the same as ambient pressure?

The answers to this question lie within equation 1.27 from the lab manual,

$$P_0 = P_s + \frac{1}{2}\rho_s v_s^2. \quad (1.27)$$

where P_0 is stagnation pressure (also called total pressure), P_s is static pressure, and the last term represents dynamic pressure. The total pressure of the system is conserved. Outside the tunnel, ambient pressure is equal to static pressure, as there is no dynamic component (assuming no velocity). If the tunnel is to generate flow, there must be a pressure difference to drive this, and inside the static must be lower than the ambient pressure in order to drive air through. Total pressure must still be conserved, and this is seen with the introduction of the dynamic pressure component, which is now present in the tunnel due to the velocity of the air. Therefore, the static pressure must be lower than ambient, and the stagnation pressure must be higher than ambient. These relationships are also evident in the small cylinder data at 30 m/s shown in figure 5-1.

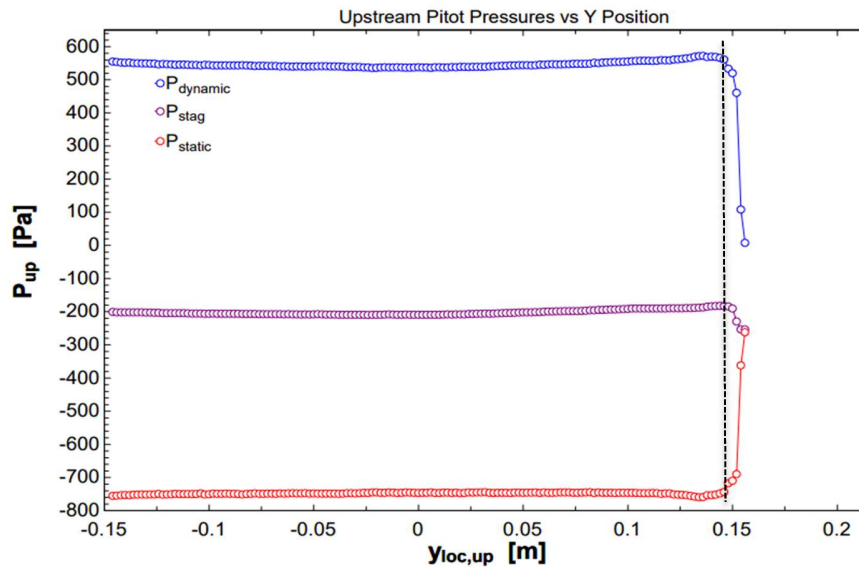


Figure 5-1. Dynamic, stagnation, and static upstream pressures as functions of vertical (y) location, as measured by the upstream pitot tube (black dotted line denotes boundary layer).

6. Explain the dynamic, static, and total pressure distributions. In what ways are the dynamic and static pressure distributions similar or different from those shown in Figure (1.6)? Describe the physical phenomenon at the top and bottom of the test section.

The dynamic, static, and total pressure distributions for the small cylinder at 30 m/s are seen in figure 5-1. Upstream, the pressure profiles make sense: total pressure must be conserved, and with flowing fluid characterized by the presence dynamic pressure, the static pressure must drop to maintain the total pressure. This drops enough so that the static pressure is below zero, indicating a pressure differential from ambient that drives the airflow.

Downstream, the pressure distributions also make sense, showing the impact the cylinder has on the fluid flow. Figure 6-1 is based on the small cylinder data at 30 m/s.

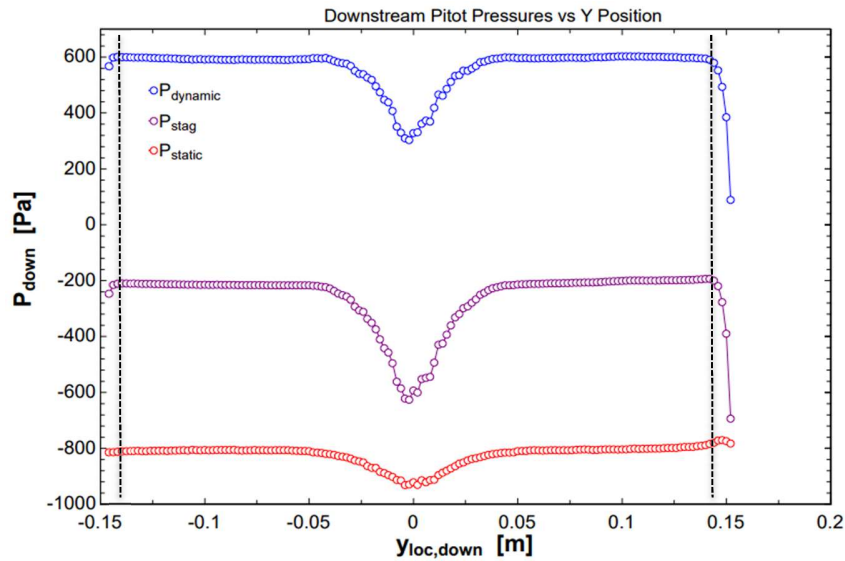


Figure 6-1. Dynamic, stagnation, and static downstream pressures as functions of vertical (y) location, as measured by the downstream pitot tube (dotted lines denote boundary layers).

Close to the center of the stream, we see dips in all three pressures. This represents the cylinder, and is expected, as it blocks fluid flow from that region of the tunnel. Compared to figure 1.6 in the lab manual, this is spot-on, as a dip in pressure distribution is also observed after the cylinder.

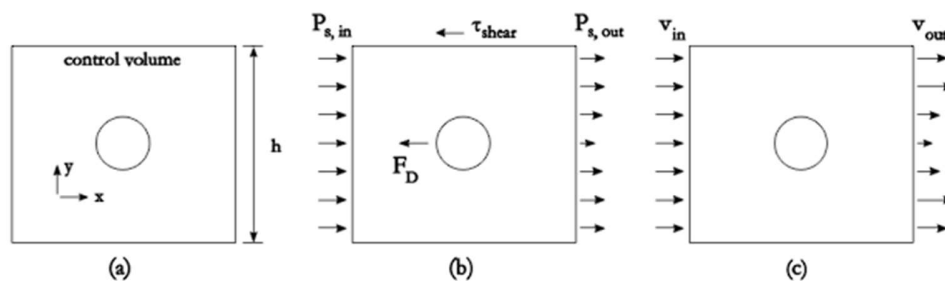


Figure 1.6: Force and momentum fluxes for flow around a cylinder. a) Control volume, b) Forces along the x -axis, c) velocity profiles.

The phenomenon at the top and bottom of the test section is the boundary layer. Boundary layers occur due to the no-slip condition at the fluid-surface interface. It takes time (and distance) into a free stream of fluid to develop velocity, so the farther air particles are from the wall, the closer their velocity is to that of the free stream. This is the drop off shown on either end of both figures 5-1 and 6-1, denoted by black dotted lines. It is worth noting that the boundary layer on the left side of the graphs is not so obvious, as the pitot probe was unable to go completely through the bottom of the test unit, as it could on the top.

7. Compare the drag force obtained using the two different methods. Can the viscous contribution to drag on the cylinder be neglected for a cylinder in crossflow?

The drag force values over the small cylinder for the pressure distribution and momentum flux methods are summarized in table 7-1.

Table 7-1. Small and cylinder drag force values obtained by various methods.

Pressure Distribution: F_d [N]	Momentum Flux: F_d [N]
3.7	4.0

A sanity check was done by hand, shown in Appendix C, confirming the validity of these drag force numbers. Additionally, for the large cylinder, the drag force was calculated to be around 8 N, with similar variation between methods.

The minor difference in methods shows that the viscous contribution to drag on the cylinder can be neglected, as the results vary by about 5%. Additionally, the uncertainty due to the shear force term in the momentum flux method could lead to higher propagated uncertainties in the calculation.

8. Compare calculated drag coefficients with values found in Figure (1.5). What are the effective length-to-diameter ratios of your cylinders?

The dimensions for both small and large cylinders are given in the lab manual and are shown in table 8-1.

Table 8-1. Dimensions of small and large cylinders.

Cylinder Size	Length [in]	Diameter [in]	Length ratio, L/d [-]
Small	12	0.75	16
Large	12	2.0	6

Using the length ratios, we are able to determine what the drag coefficients *should* be. In figure 1.5 from the lab manual, the length ratios are only listed for flow that can travel around the ends of the cylinder, which in this experiment is not the case - the ends are flush with the wall.

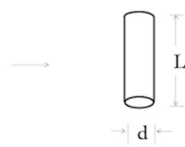
Type of Body	Length Ratio	Re	C_D
	$L / d = 1$	$10^3 - 10^5$	0.63
	$L / d = 5$	$10^3 - 10^5$	0.80
	$L / d = 10$	$10^3 - 10^5$	0.83
	$L / d = 20$	$10^3 - 10^5$	0.93
	$L / d = 30$	$10^3 - 10^5$	1.00
	$L / d = \infty$	$10^3 - 10^5$	1.20

Figure 1.5: Drag coefficients

Therefore, the *effective* length ratio is actually infinity. This last row on the table is only valid for Re between $10^3 - 10^5$, and since the laminar flow exhibited by the small cylinder has Re values within that range (table 3-1), we can expect a C_D of 1.2. As for the large cylinder, figure 1.4 from the lab manual must be examined.

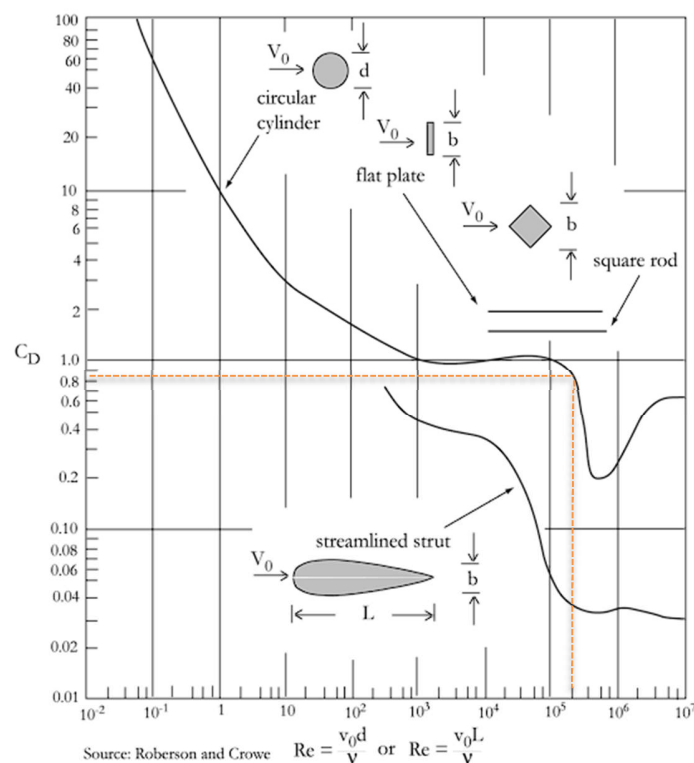


Figure 1.4: Drag coefficient for two-dimensional bodies



Following the upper curve for two-dimensional flow over a cylinder, narrowing in on the Re calculated (table 3-1), a C_D of just above 0.8 is determined (denoted by the orange dotted lines). The drag coefficients calculated from experimental data yielded very similar results, shown in table 8-2.

Table 8-2. Average drag coefficients obtained for small and large cylinders.

Cylinder Size	C_D , avg
Small	1.22
Large	0.76

9. Identify the sources of error in values of C_D . Which is most significant?

The primary sources of error in this experiment came from the uncertainties in the pressure sensors, angle measurements made by the encoder, and human error. The only official uncertainty data given was for the pressure sensors, however, leading us to believe that these were the most significant source. We do acknowledge that lack of consistency between runs, rotational speeds, and wear on the cylinders likely contributed to the overall uncertainty. The absolute and relative uncertainties in the C_D calculations are shown in table 9-1 along with the relative uncertainties for each method as the final row.

Table 9-1. Drag coefficient values and their respective uncertainties.

	Pressure Distribution Method	Momentum Flux Method
$C_{D, \text{small}}$ +/- abs. uncertainty	1.197 +/- 0.004	1.242 +/- 0.012
$C_{D, \text{large}}$ +/- abs. uncertainty	0.768 +/- 0.003	0.743 +/- 0.013
Avg. Relative Uncertainty	0.2%	1.3%

As discussed in question 7, the larger relative uncertainty seen with the momentum flux method is likely due to the shear force term and factoring in fluid viscosity.

Conclusions

Throughout the course of this experiment, we explored the behavior of fluids by using a wind tunnel as a testing apparatus. Intersecting the center of the wind tunnel was a cylinder, placed to observe how it affected the fluid flow. Both small and large cylinders were used to draw conclusions. Additionally, pitot probes, both upstream and downstream of the cylinder, were used to determine the pressure distributions. These measurements were then subjected to various analysis methods, using both the pressure distribution and momentum flux methods to derive the resultant drag coefficients across the cylinders.

As the experiment progressed, it became apparent that each method brought its own sources of error, outlined within the report. The ultimate goal was to achieve similar resultant drag coefficients between the two methods. Due to limitations posed by the test equipment, the coefficients produced by the two methods were marginally different, but not by more than 5%. Each approach makes different assumptions, and it was determined that the pressure distribution method was simpler and just as accurate.

It was concluded that careful handling of shared equipment is definitely necessary in order to maintain the accuracy of results for future lab groups. The cylinders were notably sensitive to changes in surface roughness, demonstrating the importance of minimizing unintended contact, since even minor inaccuracies could reverberate and increase the margin of error. Nevertheless, despite these minor deviations from the correct coefficients, this experiment was able to show the pros and cons of each method. Through their application, a deeper understanding of fluid mechanics was attained.

Appendices

Appendix 1: Team Contract

ME370 - Team Contract

Group (circle): A B C **D** Lab day and time: **T/Th 10-12**

This contract spells out the ground rules that everyone in the team agrees to follow when working on ME370 labs. For each category below, write 2-3 rules that you agree to follow as a group. At the end of each experiment, you will be asked to evaluate your teammates' participation using the rules in this contract as a basis. You may not get all the rules right the first time, or your group expectations may evolve over time so keep updating the contract regularly. With each deliverable for the class, you, as a group, will submit an updated version of the contract with a brief explanation of any changes made, if needed.

Participation: We agree to...

- a. **Contribute evenly**
- b. **Do each part of lab together**

Communication: We agree to...

- a. **Communication via text**
- b. **Divide work evenly**

Meetings: We agree to...

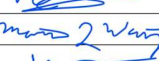

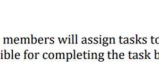
- a. **Be on time (at least by 10 min)**
- b. **Be prepared**

Conduct: We agree to...

- a. **Respect each other**
- b. **Be safe in lab**
- c. **Respect ideas/don't talk over**

Deadlines: We agree to...

- a. **Attend presentations**
- b. **Turn in on time**

Team Member's Name	Team Member's Signature
Josie	
Ethan	
Matthew	
Eric	

Non-exhaustive list of examples:

Participation:

- At the beginning of each experiment, group members will assign tasks to each individual students. Each student is responsible for completing the task by the group's deadline. Each student is responsible for asking for help with task completion if needed ahead of time.
- Everyone should review the deliverable before it is due to the instructor.

Communication:

- Communication will be done via [email, whatsapp group, choose your own].
- Communication should involve all the members of the group.
- Questions will be answered within 24 hours.

Meetings:

- We will meet regularly on [days] and [hours]
- If a student cannot make it to a meeting, they should let the other members know as soon as possible and provide a written update/list of questions if possible.
- All group members will remain in the meeting until (a) all tasks for that meeting are completed, or (b) there is unanimous adjournment.

Conduct:

- The group will actively seek a consensus based on the opinions of every member.
- Each member will take turns listening as well as talking, and active listening will be a strategy for all group discussions.
- Sexist and racist remarks are not acceptable.
- Aggressive or dominating behavior is not acceptable.

Deadlines:

- All calculations should be completed by the third class period of each lab so we have time to check our results with the instructor.
- Although we have individual tasks, the entire group is responsible for meeting deadlines. If a student is not going to meet a deadline on a specific task, they should be honest about it and let other group members as soon as possible so they can help.
- The deliverables should be completed and ready for a final review before ??pm before the day that they are due.



Appendix 2: EES Code

```
//
//START DATA                                //START DATA                                //START DATA
$IFNOT PARAMETRICTABLE
//angle_small = lookup('small',1,'angle')
P_small = lookup('small',1,'mean pressure above inlet')
//angle_large = lookup('large',1,'angle')
P_large = lookup('large',1,'mean pressure above inlet')
//y_loc_up = lookup('pitot_up',1,'location')
P_stag_up = lookup('pitot_up',1,'mean stagnation pressure')
stdev_stag_up = lookup('pitot_up',1,'stdev_stag')
P_dyn_up = lookup('pitot_up',1,'mean dynamic pressure')
stdev_dyn_up = lookup('pitot_up',1,'stdev_dyn')
//y_loc_down = lookup('pitot_down',1,'location')
P_stag_down = lookup('pitot_down',1,'mean stagnation pressure')
stdev_stag_down = lookup('pitot_down',1,'stdev_stag')
P_dyn_down = lookup('pitot_down',1,'mean dynamic pressure')
stdev_dyn_down = lookup('pitot_down',1,'stdev_dyn')
$ENDIF

//
//CYLINDERS                                //CYLINDERS                                //CYLINDERS
$IF PARAMETRICTABLE = 'small_cyl'
//angle_small = lookup('small',TableRun#,'angle')
P_small = lookup('small',TableRun#,'mean pressure above inlet')

v_inf_avg_30 = 29.55 [m/s]
C_p_ideal_small = 1 - 4*(sin(angle_small))^2 //4
C_p_small = P_small / (0.5*rho_1*(v_inf_avg_30)^2) //5
C_p_cos_s = C_p_small*cos(angle_small) //6
P_small_cos = P_small*cos(angle_small) // for 7
F_D_small = r_small*L*(integral(P_small_cos, angle_small)) //7
$ENDIF

$IF PARAMETRICTABLE = 'large_cyl'
//angle_large = lookup('large',TableRun#,'angle')
P_large = lookup('large',TableRun#,'mean pressure above inlet')

v_inf_avg_35 = 34.3
C_p_ideal_large = 1 - 4*(sin(angle_large))^2 //4
C_p_large = P_large / (0.5*rho_1*(v_inf_avg_35)^2) //5
C_p_cos_l = C_p_large*cos(angle_large) //6
P_large_cos = P_large*cos(angle_large) // for 7
F_D_large = (r_large*L)*(integral(P_large_cos, angle_large)) //7
$ENDIF

//
//PITOTS                                //PITOTS                                //PITOTS
$IF PARAMETRICTABLE = 'pitot_up'
//y_loc_up = lookup('pitot_up',TableRun#,'location')
P_stag_up = lookup('pitot_up',TableRun#,'mean stagnation pressure')
stdev_stag_up = lookup('pitot_up',TableRun#,'stdev_stag')
//P_dyn_up = lookup('pitot_up',TableRun#,'mean dynamic pressure')
stdev_dyn_up = lookup('pitot_up',TableRun#,'stdev_dyn')

//v_inf = sqrt(2*(P_dyn_up) / rho_1) //2
//v_avg = integral(v_inf, y_loc_up) / (12 [in] *convert(in,m)) //2
//Re_D_small = (rho_1*v_inf*d_small) / mu //3
//Re_D_large = (rho_1*v_inf*d_large) / mu //3

//MOMENTUM
P_dyn_up = 0.5*rho_1*vel_up^2
P_s_in = P_stag_up - P_dyn_up
```



```

int_s_in = P_s_in * A_tunnel
int_dyn_in = P_dyn_up * A_tunnel
$ENDIF

$IF PARAMETRICTABLE = 'pitot_down'
//y_loc_down = lookup('pitot_down',TableRun#,'location')
P_stag_down = lookup('pitot_down',TableRun#,'mean stagnation pressure')
stdev_stag_down = lookup('pitot_down',TableRun#,'stdev_stag')
P_dyn_down = lookup('pitot_down',TableRun#,'mean dynamic pressure')
stdev_dyn_down = lookup('pitot_down',TableRun#,'stdev_dyn')

//MOMENTUM
P_s_down = P_stag_down - P_dyn_down
int_s_down = P_s_down * A_tunnel
int_dyn_down = P_dyn_down * A_tunnel
$ENDIF
//END DATA                                //END DATA                                //END DATA

//
//
//START CALCULATIONS                        //START CALCULATIONS                        //START CALCULATIONS
//given
P_amb = 740 [mmHg] * convert(mmHg, Pa)
T_amb = 284 [K]
A_1 = 6.25 [m^2]
A_2 = 1 [m^2]
rho_1 = density(Air, P = P_amb, T = T_amb)
mu = Viscosity(Air,T=T_amb)

//dimensions
d_small = 0.75 [in] *convert(in,m)
d_large = 2 [in] *convert(in,m)
r_small = d_small / 2
r_large = d_large / 2
L = 12 [in] *convert(in,m)
A_f_s = d_small * L
A_f_l = d_large * L
A_tunnel = L^2

//calculations
//1: P_diff for 30 & 35 m/s
P_1 = P_amb
rho_2 = rho_1
v_2 = 35 [m/s]
P_1 + 0.5*(rho_1)*(v_1)^2 = P_2 + 0.5*(rho_2)*(v_2)^2
A_1 * v_1 = A_2 * v_2
P_diff = P_1 - P_2

//
//PRESSURE DISTRIBUTION METHOD                //PRESSURE DISTRIBUTION METHOD
//2: avg free stream velocity, v_inf
//v_inf = sqrt(2*(P_dyn_up) / rho_1)
//v_avg = integral(v_inf, y_loc_up) / L
//v_inf_avg_30 = 29.55 [m/s]
//v_inf_avg_35 = 34.3 [m/s]

//3: Re for both cylinders
//Re_D_small = (rho_1*v_inf*d_small) / mu

```



```

//Re_D_large = (rho_1*v_inf*d_large) / mu
//Re_D_small = 39178
//Re_D_large = 104476

//4: ideal coefficient
//C_p_ideal_small = 1 - 4*(sin(angle_small))^2
//C_p_ideal_large = 1 - 4*(sin(angle_large))^2

//5: actual coefficients
//C_p_small = P_small / (0.5*rho_1*(v_inf_avg)^2)
//C_p_large = P_large / (0.5*rho_1*(v_inf_avg)^2)

//6: C_p *cos(theta)
//C_p_cos_s = C_p_small *cos(angle_small)
//C_p_cos_l = C_p_large *cos(angle_large)

//7: F_D
//F_D_small = r_small*L *(integral(P_small_cos, angle_small)
//F_D_large = r_large*L *(integral(P_large_cos, angle_large)
//F_D_s = 3.672 [N]
//F_D_l = 8.461 [N]

//comment this if small_cyl para table is empty
{SDOLAST
  F_D_s = MAXPARAMETRIC('small_cyl', 'F_D_small')
$ENDDOLAST}

//8: C_D
//C_D_small = F_D_s / (0.5*rho_1*(v_inf_avg_30)^2*A_f_s)
//C_D_large = F_D_l / (0.5*rho_1*(v_inf_avg_35)^2*A_f_l)

//9: uncertainty

//
//MOMENTUM FLUX METHOD          //MOMENTUM FLUX METHOD          //MOMENTUM FLUX METHOD
//10: P_dyn & velocity
//P_dyn_up = 0.5*rho_1*vel_up^2
//P_dyn_down = 0.5*rho_1*vel_down^2

//11: avg free stream velocity, v_inf
//v_inf_avg_30 = 29.55 [m/s]
//v_inf_avg_35 = 34.3 [m/s]

//12: Re_L for tunnel
//Re_L_up = rho_1 * vel_up * L / mu
//Re_L_down = rho_1 * vel_down * L / mu

//13: F_shear for tunnel
//C_f_bar = (0.074/(Re_L_up^(0.2)))
//Tau_wall = 2*(0.5*rho_1*(vel_up^2)*L*C_f_bar)

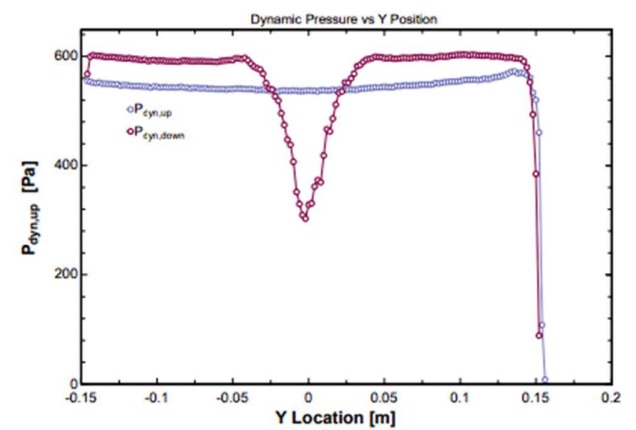
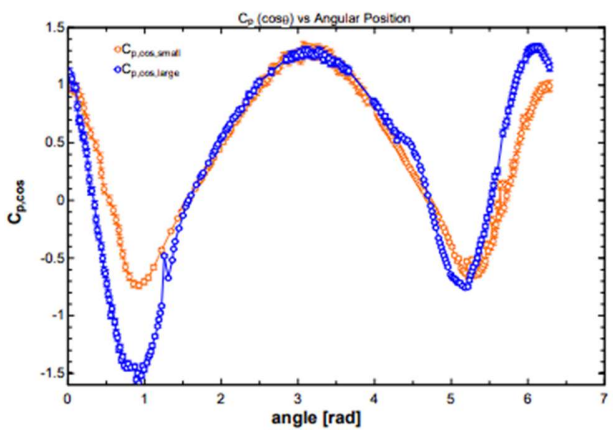
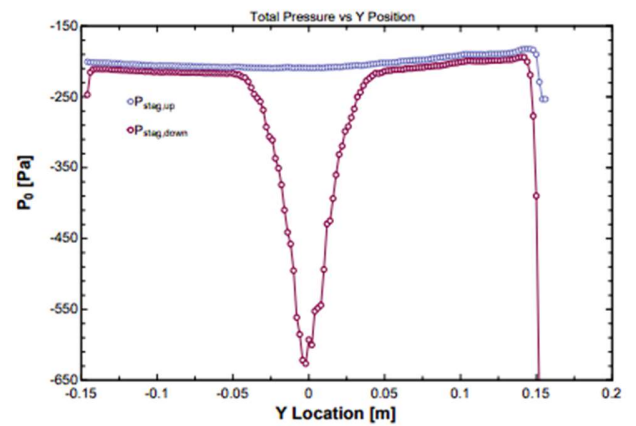
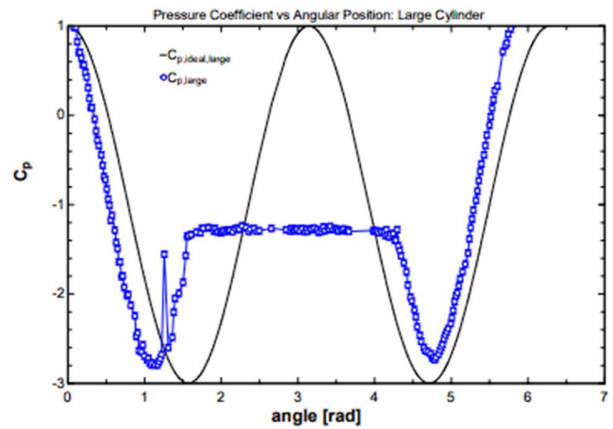
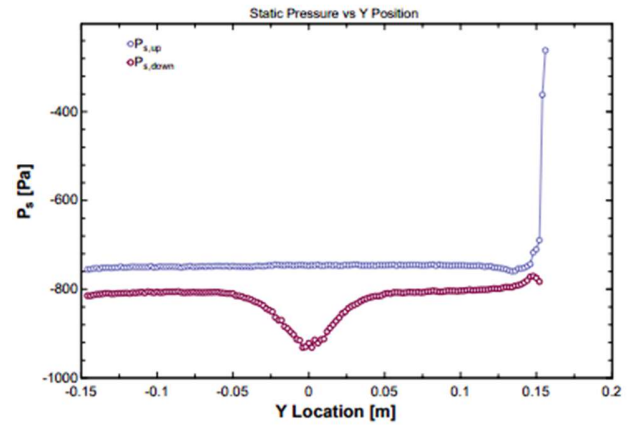
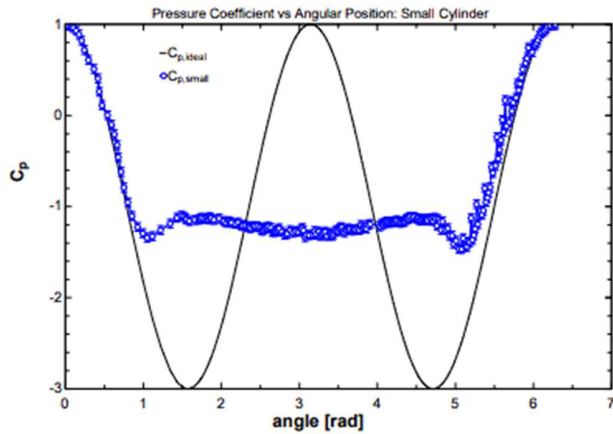
//14: F_D using 1.19
//int_s_in = P_s_in * A_tunnel
//int_s_out = integral(P_s_out, A_tunnel)
//int_dyn_in = integral(P_dyn_in, A_tunnel)
//int_dyn_out = integral(P_dyn_out, A_tunnel)
//int_s_in = -69.22 [N]
//int_s_out = -75.65 [N]

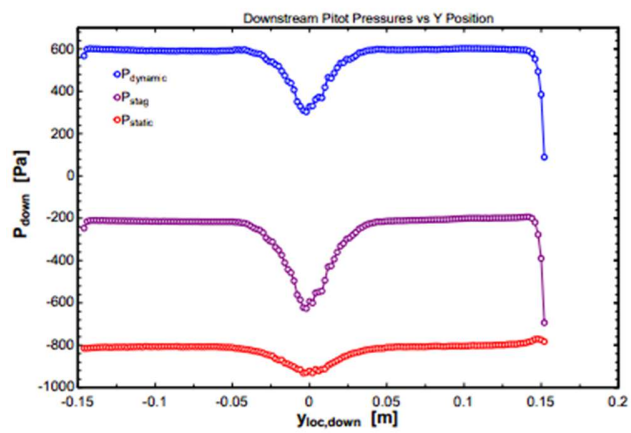
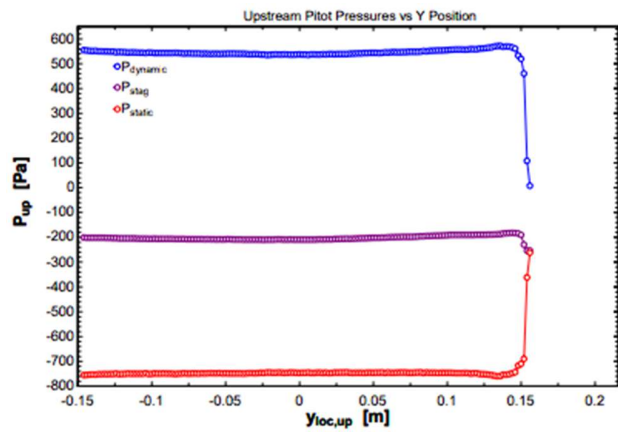
```




```
//int_dyn_in = 50.83 [N]
//int_dyn_out = 52.73 [N]
//F_D_mom = int_s_in - int_s_out - Tau_wall + int_dyn_in - int_dyn_out
```

```
//15: C_D & uncertainty
//C_D_mom = F_D_mom / (0.5*rho_1*(vel_up)^2*A_f_s)
```





Appendix 3: Hand Calculations

Calculation 1: Pressure Differential
required for 30
+ 35 m/s.

$$\text{Bernoulli's: } P_1 + \frac{1}{2}\rho_1 v_1^2 = P_2 + \frac{1}{2}\rho_2 v_2^2$$

$$P_1 - P_2 = \left[\frac{1}{2}\rho_2 v_2^2 \right] - \left[\frac{1}{2}\rho_1 v_1^2 \right]$$

$$= P_{\text{diff}}$$

$$\text{Continuity: } A_1 v_1 = A_2 v_2$$

2 eqns, 2 unknowns (v_1 + P_{diff})

$$\therefore \text{ for } 30 \text{ m/s, } P_{\text{diff}} = 530 \text{ Pa}$$

$$35 \text{ m/s, } P_{\text{diff}} = 720 \text{ Pa}$$

Calculation 7: drag force sanity check

large cylinder

C_D should be 0.8...

$$C_D = \frac{F_D}{\frac{1}{2}\rho v^2 A_{\text{ref}}} \quad (\text{eqn. 1.1})$$

$$0.8 \left(\frac{1}{2} (1.21) (30)^2 (0.015) \right) = 8.8 \text{ N}$$



Appendix 4: Citations

“Drag of Blunt Bodies and Streamlined Bodies.” Accessed: May 03, 2024. [Online].
Available: https://www.princeton.edu/~asmits/Bicycle_web/blunt.html